

## A WSe<sub>2</sub>/MoSe<sub>2</sub> heterostructure photovoltaic device

Nikolaus Flöry,<sup>1</sup> Achint Jain,<sup>1</sup> Palash Bharadwaj,<sup>1</sup> Markus Parzefall,<sup>1</sup> Takashi Taniguchi,<sup>2</sup> Kenji Watanabe,<sup>2</sup> and Lukas Novotny<sup>1</sup>

<sup>1</sup>Photonics Laboratory, ETH Zürich, Zürich 8092, Switzerland

<sup>2</sup>National Institute for Material Science, 1-1 Namiki, Tsukuba 305-0044, Japan

(Received 25 July 2015; accepted 10 September 2015; published online 22 September 2015)

We report on the photovoltaic effect in a WSe<sub>2</sub>/MoSe<sub>2</sub> heterojunction, demonstrating gate tunable current rectification with on/off ratios of over 10<sup>4</sup>. Spatially resolved photocurrent maps show the photovoltaic effect to originate from the entire overlap region. Compared to WSe<sub>2</sub>/MoS<sub>2</sub> heterostructures, our devices perform better at long wavelengths and yield higher quantum efficiencies, in agreement with Shockley-Queisser theory. © 2015 AIP Publishing LLC.

<http://dx.doi.org/10.1063/1.4931621>

Photovoltaic devices based on semiconductor p-n junctions require a judicious choice of materials that efficiently absorb solar radiation over a wide spectral range. Transition metal dichalcogenides (TMDCs) are a class of layered materials with band gaps in the range of 1–3 eV, making them ideal for optoelectronic applications including photovoltaics. Various optoelectronic devices like light emitting diodes (LEDs) and photodetectors have recently been demonstrated using TMDC-based p-n hetero- and homojunctions. For solar energy harvesting, the choice of TMDCs with different band gaps offers an unprecedented flexibility in designing the absorption profile of a p-n heterostructure to best match the solar spectrum. All existing TMDC-based p-n junction photovoltaic devices<sup>1–4</sup> use MoS<sub>2</sub> (direct band gap ~1.9 eV) as the n-type material, together with a p-type material like WSe<sub>2</sub> or WS<sub>2</sub>. On the other hand, monolayer MoSe<sub>2</sub> has a relatively low direct band gap of 1.55 eV,<sup>5,6</sup> making it well-suited for absorbing in the near-infrared (IR) part of the spectrum (Figure 1). Although vertical WSe<sub>2</sub>/MoSe<sub>2</sub> heterostructures have recently been demonstrated,<sup>7</sup> studies of electrical transport and the photovoltaic effect in such a device are still missing. In this letter, we report a MoSe<sub>2</sub>-based photovoltaic device by fabricating a WSe<sub>2</sub>/MoSe<sub>2</sub> vertical heterojunction. We show that the lower band gap of MoSe<sub>2</sub> makes the resulting device more efficient compared to a similar WSe<sub>2</sub>/MoS<sub>2</sub> p-n junction.

We fabricate our devices on a transparent glass substrate instead of the standard Si/SiO<sub>2</sub> that is used in the vast majority of reported TMDC heterostructures. A transparent substrate allows us to perform optical measurements in transmission and optical characterization that is unobstructed by the substrate. On the other hand, it requires finding transparent substitutes for the back-gate and gate-dielectric. We choose ~10 nm thick multilayer graphene (MLG) and a ~25 nm h-BN flake as the gate electrode and gate dielectric, respectively. We start our device fabrication by stacking these two on top of a glass coverslip. Next, the vertical p-n junction is built by transferring few-layer MoSe<sub>2</sub> and WSe<sub>2</sub> (3 layer thick each) on top of the h-BN, forming an overlapping region of approximately ~10 μm<sup>2</sup> as depicted in Figure 2. This back-gated configuration allows us to electrostatically tune the doping in the semiconductors while retaining optical transparency.

For electrical characterization of the fabricated devices, we added metal contacts to both TMDC layers and to the MLG backgate by e-beam lithography (EBL), followed by evaporation of 20/40 nm of palladium (Pd) and gold (Au). The high work function metal Pd serves as a good hole injector into WSe<sub>2</sub> (Ref. 8) and should provide acceptable electron injection into MoSe<sub>2</sub> at the same time.

Both the MLG backgate and the TMDC layers are connected to a Keithley digital multimeter as seen in Figure 2(a). This allows us to apply a constant gate voltage (V<sub>g</sub>) to the MLG and serves as a current source. In forward bias, electrons and holes are injected into the MoSe<sub>2</sub> (source) and WSe<sub>2</sub> (drain), respectively.

We first performed electrical measurements under different illumination intensities (λ = 633 nm, I<sub>opt</sub> = 65, 130, 190, 250, and 320 W cm<sup>-2</sup>). For studying the photocurrent I<sub>ph</sub> = I<sub>illuminated</sub> - I<sub>dark</sub>, the backgate was kept at V<sub>g</sub> = 0 V while sweeping over the drain-source voltage (V<sub>ds</sub>). The resulting I<sub>ph</sub> - V<sub>ds</sub> curves of our device are shown in Figure 3(a). Indeed, a clear photovoltaic response is observed that allows us to extract an open-circuit voltage of V<sub>OC</sub> ~ 0.46 V and an illumination dependent short-circuit current of up to

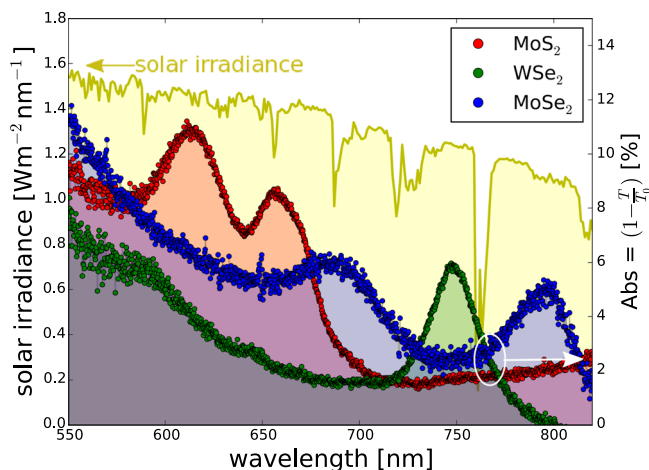


FIG. 1. Absorption in few-layer flakes of different TMDCs in comparison with the solar irradiance (AM1.5, yellow). The absorption is enhanced at the respective direct band gap energies. Of these three, MoSe<sub>2</sub> covers the broadest range in the absorption spectrum, starting at ~820 nm due to its small band gap, making it suitable for photovoltaic applications.

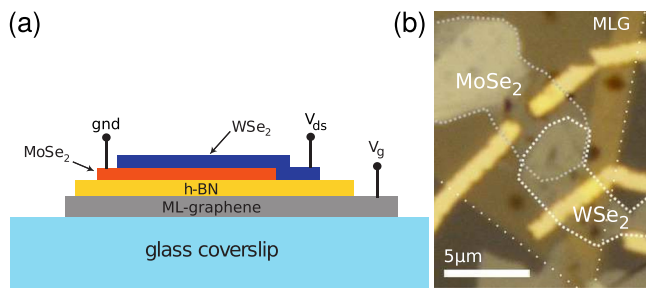


FIG. 2. (a) Schematic and (b) optical micrograph of the device showing the transparent glass substrate with a multilayer graphene and h-BN flake serving as the gate electrode and dielectric layer, respectively. On top of this stack, the MoSe<sub>2</sub> and WSe<sub>2</sub> flakes are transferred creating an overlapping junction. Metal contacts (Pd/Au) are added for electrical characterization.

$I_{SC} > 0.04$  nA for this device. The rather low fill factor, defined as the ratio of the product of the current and the voltage at the maximum power output and the product of  $I_{SC}$  and  $V_{OC}$ , could be a result of a large series resistance in our device, originating from the TMDC/metal contacts and the intrinsic TMDCs.<sup>10</sup>

To verify the origin of the photocurrent, a map was recorded at zero bias conditions ( $V_g = V_{ds} = 0$  V) by measuring  $I_{SC}$  while scanning the laser spot across the device. As illustrated in Figure 3(b), we observe a high photocurrent from the entire overlap region. This indicates the formation of a vertical junction with strong interlayer coupling, in addition to the PL spectra that show the existence of interlayer excitons (data not shown). We therefore conclude that the observed photocurrent is a result of charge separation at the junction from absorbed photons in the heterostructures.

Next,  $I_{ds} - V_{ds}$  curves were repeated in the dark. For this experiment, the MLG served as a backgate to adjust the doping level in the TMDC layers. Figure 4(a) presents the drain-source current ( $I_{ds}$ ) plotted against the drain-source voltage ( $V_{ds}$ ) for different gate voltages  $V_g$ . A strong tunability of  $I_{ds}$  is observed showing excellent current rectification with on/off ratios of more than  $10^4$ , limited only by the range of  $V_g$ , which we restrict ourselves to  $-3$  V  $< V_g < +3$  V to avoid gate leakage currents.

The diode behavior becomes stronger for negative gate voltages ( $V_g < 0$  V), with a large current flowing under

forward bias ( $V_{ds} > 0$  V) when WSe<sub>2</sub> is positively biased with respect to MoSe<sub>2</sub>. Higher negative gate voltages increase the p-doping in the WSe<sub>2</sub> and hence result in an increased current. The observed IV characteristics are similar to those of reported p-WSe<sub>2</sub>/n-MoS<sub>2</sub> devices.<sup>1,2</sup> Additional measurements were performed on a second device with two independent contacts on each flake. The observed ambipolar transport suggests that the rectifying behavior stems from an asymmetric p-p junction rather than from a true p-n junction.

In contrast to this rectifying behavior, a different regime is found for positive gate voltages ( $V_g > 0$  V). In this range, the magnitude of  $I_{ds}$  in forward bias is not as high as for  $V_g < 0$  V, which is consistent with a suppression of the p-type behavior in WSe<sub>2</sub> that limits the transport. Under strong reverse bias ( $V_{ds} < 0$  V), however,  $I_{ds}$  increases for  $V_g > 0$  V, as seen in Figure 4(b), displaying a “backward-diode” behavior. This sharp rise in  $I_{ds}$  suggests vertical band-to-band electron tunneling (BTBT) as a possible origin, as it was recently observed in other van der Waals heterostructures.<sup>9</sup>

In order to directly compare the optoelectronic properties of our WSe<sub>2</sub>/MoSe<sub>2</sub> heterojunction with MoS<sub>2</sub> based devices reported recently,<sup>1-4</sup> we also fabricated a device by replacing MoSe<sub>2</sub> with MoS<sub>2</sub>, keeping everything else the same. Transmission of the two devices was measured using a white light source (NKT SuperK Extreme). Reference spectra were taken by focusing the beam on an area with just the MLG gate and the h-BN layer, and these spectra were then used to normalize the transmission through the junctions. As expected, the absorption spectra of both the WSe<sub>2</sub>/MoS<sub>2</sub> and WSe<sub>2</sub>/MoSe<sub>2</sub> devices exhibit peaks at the corresponding exciton energies of their TMDC components (Figure 5). The indirect band gap does not play a significant role, despite the fact that the used TMDC layers are not monolayers. This is because the absorption cross-section at the indirect band gap is much smaller than at the direct band gap energy.

Because of their different TMDC compositions, the two different heterostructures absorb in partially different wavelength ranges. In particular, our WSe<sub>2</sub>/MoSe<sub>2</sub> junction shows a high absorption in the range  $675$  nm  $< \lambda < 725$  nm and  $775$  nm  $< \lambda < 820$  nm, regions where the WSe<sub>2</sub>/MoS<sub>2</sub> junction is only able to collect a smaller fraction of the incident photons. Figure 5 also shows external quantum efficiency

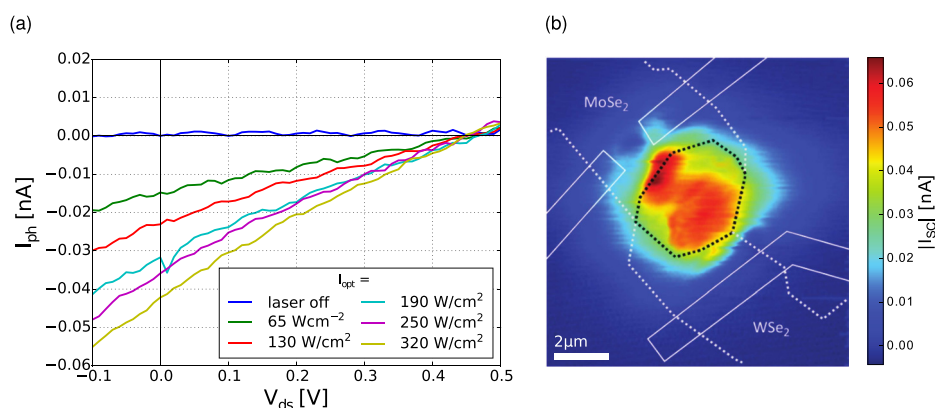


FIG. 3. Electrical characteristics of our WSe<sub>2</sub>/MoSe<sub>2</sub> device under illumination. (a)  $I_{ph} - V_{ds}$  curves taken at  $V_g = 0$  V for different illumination intensities ( $I_{opt} = 65, 130, 190, 250,$  and  $320$  W cm<sup>-2</sup>). A constant open circuit voltage of  $V_{OC} \sim 0.46$  V can be extracted, whereas the short circuit current increases with illumination power up to  $I_{SC} > 0.04$  nA. (b) Photocurrent-map recorded at  $V_g = V_{ds} = 0$  V. A strong photocurrent is originating from the entire overlapping area indicating the formation of a vertical junction with high interface quality.

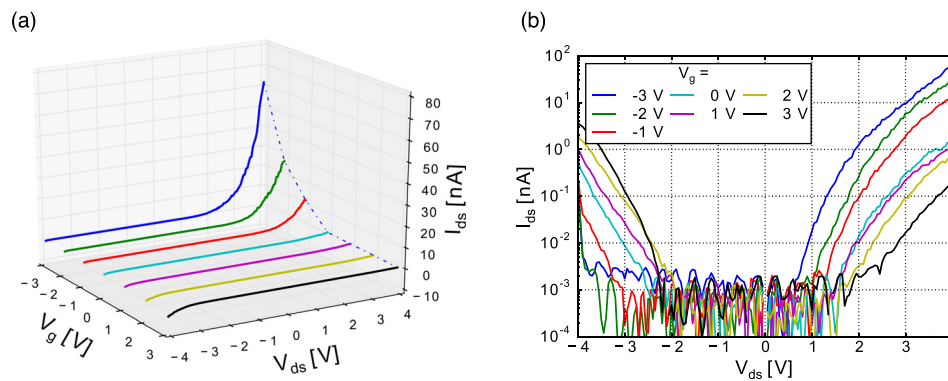


FIG. 4. Electrical characterization of a  $\text{WSe}_2/\text{MoSe}_2$  heterojunction. (a) Several  $I_{\text{ds}} - V_{\text{ds}}$  curves in the dark for different gate voltages. A strong rectification is visible at negative gate voltages  $V_{\text{g}} < 0 \text{ V}$  in forward bias  $V_{\text{ds}} > 0 \text{ V}$ . (b) The same data as in (a), but plotted on a logarithmic scale. In forward bias for  $V_{\text{g}} < 0 \text{ V}$ , we see normal diode like behavior, whereas in reverse bias and for  $V_{\text{g}} > 0 \text{ V}$ , the device acts like a “backward-diode” with a sharp increase in  $I_{\text{ds}}$ .

(EQE) calculations from photocurrent measurements that were performed by selecting various wavelengths of the supercontinuum source (with optical intensities between  $I_{\text{opt}} = 20$  and  $430 \text{ W cm}^{-2}$ ). These measurements indicate that contributions to the photocurrent come from partly different spectral regions, in good agreement with the absorption spectra of the corresponding devices. Especially between  $750 \text{ nm} < \lambda < 850 \text{ nm}$ , a much higher EQE from the  $\text{WSe}_2/\text{MoSe}_2$  device is observed than for the  $\text{WSe}_2/\text{MoS}_2$  junction, highlighting the advantage of the smaller band gap of  $\text{MoSe}_2$ . Taking into account the solar spectrum, this leads to an overall enhancement of the EQE by a factor of  $\sim 5$  for our  $\text{MoSe}_2$  based device. Moreover, these observations clearly show the usefulness and advantages of a device that could be made combining three TMDCs in a single device to significantly broaden the absorption spectrum, and to hence enhance the current conversion efficiency.

In summary, we have fabricated and investigated the electrical characteristics of a vertical  $\text{WSe}_2/\text{MoSe}_2$  heterostructure on a transparent glass substrate. We demonstrate

good current rectification in forward bias and observe a “backward-diode” behavior in reverse bias, both of which can be tuned by an applied gate voltage. A photovoltaic response from the overlap region of the heterostructure is observed. Due to the transparency of our devices, we are able to measure the absorption spectrum as well as the photoresponse and provide a quantitative comparison with similar  $\text{WSe}_2/\text{MoS}_2$  devices. The  $\text{MoSe}_2$  device shows an enhancement of absorption and photocurrent generation over a reference  $\text{WSe}_2/\text{MoS}_2$  device. We emphasize that the weak absorption and low EQE are the result of using  $\text{MoSe}_2$  that is only three layers thick. To increase the absorption and the EQE near unity levels, the TMDC thicknesses need to be increased considerably. Our results show that the spectral behavior of photovoltaic devices can be tailored by a proper choice of TMDC materials and hence can be made to best suit given environmental conditions.

*Note added:* During the finalization of this manuscript we became aware of a related study.<sup>11</sup>

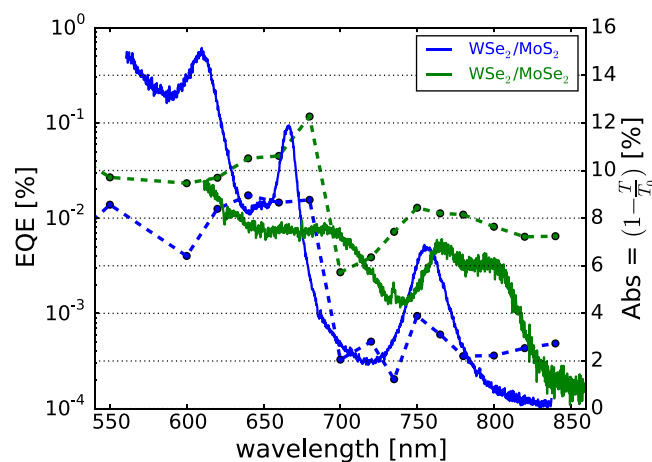


FIG. 5. Absorption (solid lines) and EQE measurements (dashed lines) for a  $\text{WSe}_2/\text{MoS}_2$  and a  $\text{WSe}_2/\text{MoSe}_2$  device. Both heterostructures show high absorption at the exciton energies at the band gaps of their corresponding TMDC compounds. Our  $\text{WSe}_2/\text{MoSe}_2$  device shows a rather high absorption already starting at  $\sim 820 \text{ nm}$ , as a result of the small band gap of  $\text{MoSe}_2$ . Additionally, EQE measurements were performed at different wavelengths that are in good agreement with the absorption spectra, attesting a higher photocurrent for higher wavelengths for our  $\text{WSe}_2/\text{MoSe}_2$  junction compared to the  $\text{WSe}_2/\text{MoS}_2$  junction.

This work was supported by the NCCR-QSIT program (Grant No. 51NF40 160591) and the Swiss National Science Foundation (Grant No. 200021 149433). We also acknowledge the use of facilities at the FIRST Center for Micro- and Nanotechnology as well as the Scientific Center for Optical and Electron Microscopy (ScopeM) at ETH Zürich.

<sup>1</sup>M. Furchi, A. Pospischil, F. Libisch, J. Burgdörfer, and T. Mueller, “Photovoltaic effect in an electrically tunable van der Waals heterojunction,” *Nano Lett.* **14**, 4785–4791 (2014).

<sup>2</sup>C.-H. Lee, G.-H. Lee, A. M. van der Zande, W. Chen, Y. Li, M. Han, X. Cui, G. Arefe, C. Nuckolls, T. F. Heinz, J. Guo, J. Hone, and P. Kim, “Atomically thin p-n junctions with van der Waals heterointerfaces,” *Nat. Nanotechnol.* **9**, 676–681 (2014).

<sup>3</sup>R. Cheng, D. Li, H. Zhou, C. Wang, A. Yin, S. Jiang, Y. Liu, Y. Chen, Y. Huang, and X. Duan, “Electroluminescence and photocurrent generation from atomically sharp  $\text{WSe}_2/\text{MoS}_2$  heterojunction pn diodes,” *Nano Lett.* **14**, 5590–5597 (2014).

<sup>4</sup>H. Fang, C. Battaglia, C. Carraro, S. Nemsak, B. Ozdol, J. S. Kang, H. A. Bechtel, S. B. Desai, F. Kronast, A. A. Unal, G. Conti, C. Conlon, G. K. Palsson, M. C. Martin, A. M. Minor, C. S. Fadley, E. Yablonovitch, R. Maboudian, and A. Javey, “Strong interlayer coupling in van der Waals heterostructures built from single-layer chalcogenides,” *Proc. Natl. Acad. Sci. U.S.A.* **111**, 6198–6202 (2014).

<sup>5</sup>S. Tongay, J. Zhou, C. Ataca, K. Lo, T. S. Matthews, J. Li, J. C. Grossman, and J. Wu, “Thermally driven crossover from indirect toward direct bandgap in 2D semiconductors:  $\text{MoSe}_2$  versus  $\text{MoS}_2$ ,” *Nano Lett.* **12**, 5576–5580 (2012).

- <sup>6</sup>A. Kumar and P. Ahluwalia, "Electronic structure of transition metal dichalcogenides monolayers 1H-MX<sub>2</sub> (M=Mo, W; X=S, Se, Te) from *ab-initio* theory: New direct band gap semiconductors," *Eur. Phys. J. B* **85**, 186 (2012).
- <sup>7</sup>P. Rivera, J. R. Schaibley, A. M. Jones, J. S. Ross, S. Wu, G. Aivazian, P. Klement, K. Seyler, G. Clark, N. J. Ghimire, J. Yan, D. G. Mandrus, W. Yao, and X. Xu, "Observation of long-lived interlayer excitons in monolayer MoSe<sub>2</sub>-WSe<sub>2</sub> heterostructures," *Nat. Commun.* **6**, 6242 (2015).
- <sup>8</sup>H. Fang, S. Chuang, T. C. Chang, K. Takei, T. Takahashi, and A. Javey, "High-performance single layered WSe<sub>2</sub> p-FETs with chemically doped contacts," *Nano Lett.* **12**, 3788–3792 (2012).
- <sup>9</sup>T. Roy, M. Tosun, X. Cao, H. Fang, D.-H. Lien, P. Zhao, Y.-Z. Chen, Y.-L. Chueh, J. Guo, and A. Javey, "Dual-gated MoS<sub>2</sub>/WSe<sub>2</sub> van der Waals tunnel diodes and transistors," *ACS Nano* **9**, 2071–2079 (2015).
- <sup>10</sup>M. Li, Y. Shi, C. Cheng, L. Lu, Y. Lin, H. Tang, M. Tsai, C. Chu, K. Wei, J. He, W. Chang, K. Suenaga, and L. Li, "Epitaxial growth of a monolayer WSe<sub>2</sub>-MoS<sub>2</sub> lateral p-n junction with an atomically sharp interface," *Science* **349**, 524–528 (2015).
- <sup>11</sup>Y. Gong, S. Lei, G. Ye, B. Li, Y. He, K. Keyshar, X. Zhang, Q. Wang, J. Lou, Z. Liu, R. Vajtai, W. Zhou, and P. M. Ajayan, "Two-step growth of two-dimensional WSe<sub>2</sub>/MoSe<sub>2</sub> heterostructures," *Nano Lett.* **15**, 6135–6141 (2015).